

On direct observation of millicharged particles at $c\text{-}\tau$ factories and other e^+e^- -colliders

Dmitry Gorbunov^{a,b}, Dmitry Kalashnikov^{a,b}, Pavel Pakhlov^{c,d}, Timofey Uglov^{c,b}

^a*Institute for Nuclear Research of Russian Academy of Sciences, 117312 Moscow, Russia*

^b*Moscow Institute of Physics and Technology, 141700 Dolgoprudny, Russia*

^c*P.N. Lebedev Physical Institute of the RAS, Moscow, Russia*

^d*Higher School of Economics (National Research University), Moscow, Russia*

Abstract

Hypothetical particles with tiny electric charges (millicharged particles or MCPs) can be produced in electron-positron annihilation if kinematically allowed. Typical searches for them at e^+e^- colliders exploit a signature of a single photon with missing energy carried away by the undetected MCP pair. We put forward an idea to look alternatively for MCP energy deposits inside a tracker, which is a direct observation. The new signature is relevant for non-relativistic MCPs, and we illustrate its power on the example of the $c\text{-}\tau$ factory. We find that it can probe the MCP couplings down to 3×10^{-3} of the electron charge for the MCP masses in $\mathcal{O}(5)$ MeV vicinity of each energy beam value where the factory will collect a luminosity of 100 fb^{-1} .

1. Feebly Interacting Massive Particles (FIMPs) is one of the options considered in various extensions of the Standard Model of particle physics (SM). The SM extensions are intended to explain the dark matter phenomena, baryon asymmetry of the Universe, neutrino oscillations, and other issues which the SM fails to describe. While the name FIMPs had been suggested for dark matter candidates with coupling to SM particles much weaker than that of WIMPs (weakly interacting massive particles), see e.g. [1, 2], afterward it was used for non-dark matter candidates as well (and sometimes replaced by FIPs for Feebly Interacting Particles, see e.g. [3]). A natural example of FIMPs is provided by so-called millicharged particles (MCPs)—hypothetical particles with tiny electric charge—which are predicted in SM extensions with vector portal coupling(s) to the hidden sector(s) [4], and are generically allowed with Abelian gauge subgroups popped up at high energies.

The tiny electric charge provides stability to the MCPs and, hence, makes them a natural candidate for dark matter [5]. Anyway, if present, MCPs can impact on cosmology as a (main) part of dark matter sector [6, 7], boost the star evolution and supernova explosion as

Email addresses: gorby@ms2.inr.ac.ru (Dmitry Gorbunov), kalashnikov.d@phystech.edu (Dmitry Kalashnikov), uglov.timofey@gmail.com (Timofey Uglov)

additional source of cooling [8–10], induce the muon $g - 2$ anomaly [11], explain the EDGES signal at 21 cm [12, 13], etc. Direct searches for MCPs have been performed in cosmic rays, at particle colliders, and at beam dump experiments, in experiments investigating neutrino physics, see e.g. Ref. [14] for a review and Fig.5.9 of Ref. [15] for the most recent summary of experimental constraints on the charge and mass of MCP.

In this letter, we discuss MCP searches at e^+e^- colliders, where they can be directly produced in pairs by a virtual photon thanks to their non-zero electric charge. Produced MCPs having a small charge $\epsilon \ll 1$ (in terms of the electron charge e) practically do not interact with the detector material and freely escape any detection. Since at e^+e^- colliders initial 3-momenta are fixed, as a MCP signature the missing energy (taken away by MCPs) and a single photon (emitted by the colliding leptons) is generally adopted. This signature has been widely used in MCP searches at e^+e^- colliders; the obtained limits are from e.g. LEP-I [16], LEP-II [17], BESS-III [18], BaBar [19]. It will be also exploited in future searches at Belle II [19] and developing projects like τ - c factory [19] and CEPC [20].

2. Here we propose another signature, which for e^+e^- colliders, as we show below, turns out to be more sensitive to models with MCP (as compared to the traditional missing energy), but is applicable to rather limited regions in the model parameter space: namely, for the MCP mass m_χ close to the half of the e^+e^- collision energy $\sqrt{s}/2 \approx m_\chi$. In this case, despite the smallness of the electric charge, MCPs are non-relativistic and still able to produce hits in the tracker either by ionization or by knocked-on δ -electrons. A hit probability is very small, thus a full-fledged track is unfeasible. However, the MCPs hits pattern will be so distinctive that it will be possible to identify the process under the study without background.

Indeed, tracks of even non-relativistic MCPs are almost unbent by the detector magnetic field: the maximum declination from the straight line is comparable with the tracker resolution. Moreover, two MCPs are produced back-to-back, thus their hits must be on the straight line crossing the interaction point. Such a signature cannot be imitated by background processes. We propose to consider as MCPs signature more or equal to four hits from both MCPs in the event, with at least one hit from each MCPs. There is no physical background that can produce such a subtrack, while the probability of the coincidence for four random hits to lie on the same line is negligibly small with a typical background rate. Another important issue for the ability to register this process is also the possibility of finding the proposed signature at the trigger level. A simple finder of four or more hits positioned along the straight line passing through the interaction point could be easily implemented at all trigger levels. The combinatorial background that still can randomly generate similar pattern can be effectively controlled with the random trigger data.

So we look at the direct production of MCPs close to their threshold,

$$e^+ + e^- \rightarrow \chi + \bar{\chi},$$

where they are essentially non-relativistic, with velocity

$$\beta \equiv \sqrt{\frac{\sqrt{s}}{m_\chi} - 2} \ll 1.$$

Hence their total production cross section is given by

$$\sigma_{e^+e^- \rightarrow \chi\bar{\chi}}(s) = \frac{2\pi\alpha^2\epsilon^2\beta}{s}, \quad (1)$$

which can be rescaled from that of muon pair production at the threshold.

Since the center of mass energy is not exactly monochromatic due to a beam energy smear, we approximate it by the Gaussian shape with mean value $\sqrt{s_0}$ and dispersion σ_0^2 . If the collider operates for some time at a given energy $\sqrt{s_0}$ and collects an integrated luminosity \mathcal{L}_0 , the effective differential luminosity is

$$dL = \frac{\mathcal{L}_0}{\sqrt{2\pi}\sigma_0} \times \exp\left(-\frac{(\sqrt{s} - \sqrt{s_0})^2}{2\sigma_0^2}\right) d\sqrt{s} \quad (2)$$

and the total mass of the produced at this operation period MCP pairs can be estimated as

$$N(\sqrt{s_0}) = \int d\sqrt{s} \frac{dL}{d\sqrt{s}} \sigma_{e^+e^- \rightarrow \chi\bar{\chi}}(s). \quad (3)$$

The beam energy dispersion significantly reduces the production of non-relativistic MCP of a particular mass but instead extends the MCP production inside a mass range $m_\chi = \sqrt{s_0}/2 \pm \sigma_0$. Initial State Radiation (ISR) leads to a similar effect, but as we show in due course, the ISR contribution in comparison to the beam energy smearing can be neglected in this respect.

3. The produced MCPs are stable but can interact inside the tracker (which is typically the closest to the collision point part of the main detector). It has a low matter density, but a sufficiently non-relativistic MCP can ionize its material while passing through and/or kick off a δ -electron which does the same job. A few hits along the MCP path can be used to identify the MCP pair produced near the threshold.

The MCP ionization energy loss during propagating in the tracker filled with a gas of density ρ , nuclear charge Z , and atomic mass A reads (see e.g. [21])

$$\frac{dE}{dx} = \rho K \times \frac{Z}{A} \times \frac{\epsilon^2}{\beta^2} \times \frac{1}{2} \times \log \frac{2m_e\beta^2 T_{\max}}{I^2}, \quad (4)$$

where I is the effective energy of ionization, $K = 0.307 \times 10^6 \text{ eV cm}^2 \text{ mol}^{-1}$, and the maximal energy transfer from MCP to electron T_{\max} comes from the scattering kinematics as

$$T_{\max} = \frac{2m_e\beta^2\gamma^2}{1 + \frac{2\gamma m_e}{m_\chi} + \left(\frac{m_e}{m_\chi}\right)^2}. \quad (5)$$

In the limit of heavy and slow MCP one finds $T_{\max} \rightarrow 2m_e\beta^2$. To illustrate the effect, we assume the tracker filled with propane, then $Z = 26$, $A \approx 44 \text{ g mol}^{-1}$, $I \approx 11 \text{ eV}$ and $\rho = 1.864 \times 10^{-3} \text{ g cm}^{-3}$ and so eq. (4) becomes

$$\frac{dE}{dx} = 25 \frac{\text{eV}}{\text{cm}} \times \left(\frac{\epsilon}{1.8 \times 10^{-3}}\right)^2 \times \left(\frac{10^{-2}}{\beta}\right)^2. \quad (6)$$

One concludes that the small electric charge of MCP may be compensated by small velocity to make the same ionization (6) as the ordinary charged particles, e.g. electrons, do. In a realistic setup it can be observed and hence adopted as an indicator of MCP passage if the process is sufficiently intensive, i.e.

$$\frac{dE}{dx} > I_{min} \quad (7)$$

and if MCP covers a sufficient distance enable to identify the track, i.e.

$$\int dx > L_{min}. \quad (8)$$

The differential energy spectrum of δ -electrons produced per unit length dx by a travelling MCP of velocity β reads [21]

$$\frac{d^2 N_\delta}{dx dT_e} = \rho \frac{K Z \epsilon^2 F(T_e)}{2 A \beta^2 T_e^2}, \quad (9)$$

where for non-relativistic electrons one can set $F(T_e) \approx 1$. The estimate (9) is valid for MCP faster than electrons bound in atom, i.e. $\beta > \alpha$, and for sufficiently energetic MCPs. In practice, the electron energy must exceed some value,

$$T_e > T_{min}, \quad (10)$$

to be detected through the subsequent ionization. Thus the number of viable δ -electrons, which are produced by MCP covered a distance L , can be estimated as

$$N_\delta = \rho \frac{K Z \epsilon^2}{2 A \beta^2} L \left(\frac{1}{T_{min}} - \frac{1}{T_e} \right). \quad (11)$$

Recall that the kinematics limits the maximum energy transfer from MCP to the δ -electron as (5). Each MCP must kick at least two δ -electrons to trace the MCP trajectory.

4. To illustrate the efficiency of the suggested method in searches for MCP at e^+e^- colliders we perform a numerical estimate for a tracker filled with propane and choosing $\sqrt{s_0} = 3 \text{ GeV}$, $\mathcal{L}_0 = 100 \text{ fb}^{-1}$, $\sigma_0 = \sqrt{2} \times 0.1\% \times \sqrt{s_0}/2$ and so σ_0 equals 2.1 MeV. We assume that the ionization signature is reliable for identification of MCP if $I_{min} = 25 \text{ eV cm}^{-1}$, $T_{min} = 1 \text{ keV}$, $L_{min} = 10 \text{ cm}$. Alternatively, for the δ -electron signature we ask that each one of the produced MCP kicks $N_\delta = 2$ δ -electrons, and tacker is a cylinder of $L = 1 \text{ m}$ radius. The numbers are consistent with the machine parameters and the detector architecture of the $c\text{-}\tau$ factory project designed in Budker Institute of Nuclear Physics (Novosibirsk), see the project proposal at <https://sct.inp.nsk.su>.

With the chosen collider and detector parameters, one can roughly limit the attainable MCP velocities from below. For the ionization the lowest recognizable intensity (7) and shortest acceptable length (8) implies $\beta > 6 \times 10^{-4}$. The signature with δ -electrons for (5) and (10) to be fulfilled requires $\beta > 3 \times 10^{-2}$. We observe below that the relevant velocities

always exceed 0.5×10^{-2} , which is still within the borders of applicability of the energy loss formulas we use, (6), (9). The numerical analysis is accomplished by scanning over m_χ and ϵ , integrating over the beam energy spread in (3) while checking all the constraints on the velocity, imposed for the corresponding signal to be recognizable as we explained above. These constraints cut the actual range of integration in (3). Then we compare the number of obtained events with 3 corresponding to 95% CL within the Poisson statistics. If the number exceeds this value, the region around this particular point in (m_χ, ϵ) plane can be tested with our method.

The numerical results are presented in Fig.1. In the model with parameters in the upper

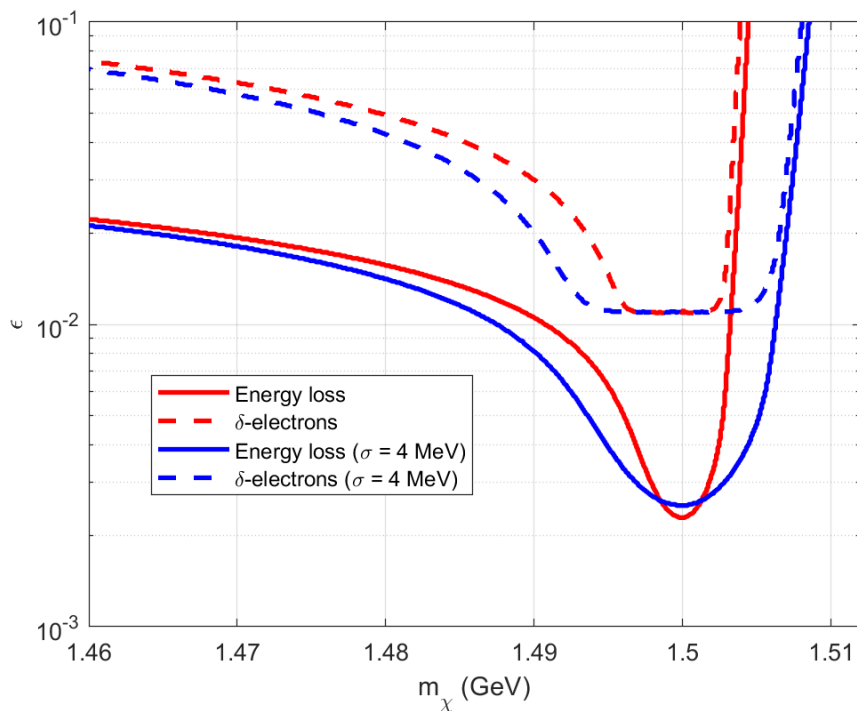


Figure 1: The outlined regions would provide with 3 or more signal events upon collecting $\mathcal{L}_0 = 100 \text{ fb}^{-1}$ integrated luminosity at collision energy $\sqrt{s_0} = 3 \text{ GeV}$, see the main text for the detector parameters. The red lines are obtained with beam energy spread $\sigma_0 = \sqrt{2} \times 10^{-3} \times \sqrt{s_0}/2 = 2.1 \text{ MeV}$ and the blue lines with $\sigma_0 = 4 \text{ MeV}$.

regions outlined by red solid (dashed) lines one expects more than 3 MCP events with ionization (δ -electron) signature described above, and the upper region will be excluded at 95% CL if no events are observed. The similar blue lines show the same limits but obtained with larger beam energy spread, $\sigma_0 = 4 \text{ MeV}$. Evidently with a broader beam energy one probes a wider MCP mass range, but the probing is poorer at the very threshold for the ionization and remains the same for δ -electrons. The latter is because the lower limit on ϵ here is related to the minimal β from (10) via (11). The range of MCP signature with δ -electron is limited from above by kinematics related to T_{min} and σ_0 . The similar kinematics works in case of ionization, but the minimal possible velocity here is lower, and so the smaller

charges are accessible. The width of the mass region where the searches exhibit the highest sensitivity is the same for both signatures, and it is determined by the beam width. The position of each region is defined by kinematics, that is the minimal accessible kinetic energy or the minimal velocity, which is somewhat different. The sensitivity to lighter MCPs are limited by the intensity limit (7) and minimal length (8) for the ionization signature and the number of kicked electrons (11) for δ -electrons.

We observe that a higher sensitivity to MCPs are exhibited by the ionization signature.

At first glance, both signatures we discuss work perfectly as far as $\epsilon \sim \beta$, see eqs. (6) and (9). Inserting this relation into the cross section (1) one finds that the requirement to have a few events with statistics of 100 fb^{-1} would imply testing the charge as low as 10^{-3} , while our numerical calculation reveals 3 times larger value. This discrepancy is due to the non-monochromaticity of the colliding beams. Indeed, the velocity 10^{-3} implies the MCP kinetic energy of 750 eV, while the 0.1% beam energy spread we use in our estimates implies the mass range of about 1.5 MeV. Hence, the production of MCP with kinetic energy below 750 eV is highly suppressed because of much lower effective luminosity. Since the number of events in the monochromatic case scales as β^3 , and the MCP kinetic energy scales as β^2 , the typical velocity of the produced MCP is by a factor $(1.5 \times 10^3 / 0.75)^{1/5} \approx 4.5$ higher than our naive estimate 10^{-3} , that nicely fits to the numerical results shown in Fig. 1.

It is worth to note that the center-of-mass energy of the colliding e^+e^- pair must be corrected for the unavoidable Initial State Radiation, which escapes detection. This can be done with the following extension of eq. (3),

$$N(\sqrt{s_0}) = \int d\sqrt{s} \int_0^{x_{max}} dx \frac{dL}{d\sqrt{s}} \sigma_{e^+e^- \rightarrow \chi\bar{\chi}}((1-x)s) H(x, s), \quad (12)$$

where the kernel $H(x, s)$ is presented in Ref. [22] and x refers to the energy fraction carried away by the emitted (and missed) photons as $x = 1 - s'/s$; the maximal fraction is taken to be $x_{max} = (25 \text{ MeV})^2/s$. We find that for the interesting energy and mass ranges the kernel can be approximated simply as

$$H(x, s) = B(x^{B-1} - 1 + x/2), \quad \text{with} \quad B = \frac{2\alpha}{\pi} \left(\log \left(\frac{s}{m_e^2} \right) - 1 \right).$$

We repeat the previous analysis and obtain the limits presented in Fig. 2. One observes that the corrections due to ISR are small and we neglect them in what follows.

The estimated sensitivity above is obtained upon zero background condition given the suggested signatures. Then, since the number of signal events scales as $N \propto \mathcal{L} \times \epsilon^2 \times \epsilon^2$, with ten times higher statistics, 1 ab^{-1} , the overall sensitivity will increase by a factor of 1.8. The sensitivity of the ionization technique can be extended to smaller masses with lower L_{min} and to bigger and smaller masses and even to smaller ϵ with lower I_{max} . Naturally the sensitivity of our signatures will be also improved with denser gas in the tracker, but this way is limited as it alters the zero background conditions.

Typically e^+e^- -machine either operates at several specially chosen collision energies $\sqrt{s_0}$ or performs a scan over some energy range. This program would allow to probe a

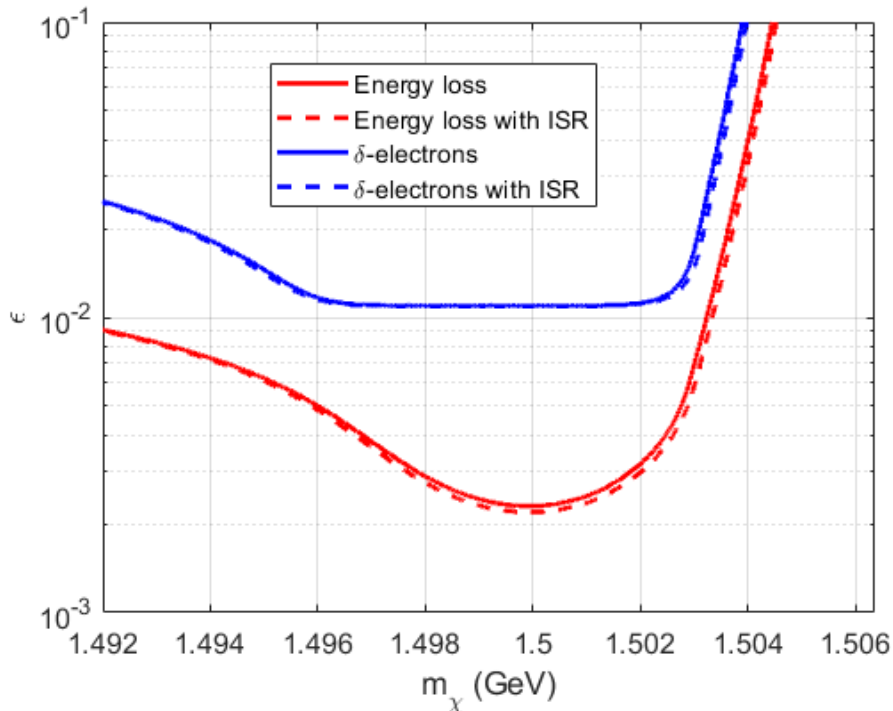


Figure 2: The outlined regions would provide with 3 or more signal events upon collecting $\mathcal{L}_0 = 100 \text{ fb}^{-1}$ integrated luminosity at collision energy $\sqrt{s_0} = 3 \text{ GeV}$, with $\sigma_0 = 2.1 \text{ MeV}$, see the main text for detector parameters. The solid lines are obtained without contribution of ISR and the dash lines with ISR.

broader region of MCP masses. To illustrate the realistic prospects we assume that the $c\text{-}\tau$ factory follows the plan to operate for one year at several energies near the thresholds of interesting hadronic resonances, see Tab.1.1 in the CDR (part one) of the proposal at <https://sct.inp.nsk.su>. The total collected luminosity is 1000 fb^{-1} . This program gives an opportunity to investigate the regions depicted in Fig. 3. There we also shade the regions excluded at 95% CL by previous searches with particle accelerators. In this respect it is worth to mention other competitive limits from analysis [25] of Super-K results and reinterpretation [26] of the results of BEBC WA66 experiment.

5. To conclude, we propound a new method to search for hypothetical millicharged particles produced in electron-positron collisions. It exploits a high ionization power of non-relativistic particles, which compensates for the smallness of their electric charge. The method enables to probe the regions of masses close to the threshold. We illustrate the perspectives of this method applying it in the framework of proposed $c\text{-}\tau$ -factory <https://sct.inp.nsk.su>. With one-year program of collecting data at certain collision energies (related to the thresholds of interesting particles) presented in Tab.1, one can be able to test the charges as small as $\epsilon \sim 3 \times 10^{-3}$.

The sensitivity can be increased with narrower beam energy of colliding particles, though it would shrink the mass range under investigation. Since the number of signal events scales as ϵ^4 , an increase in sensitivity by a factor of 2 requires 16 times longer operation period.

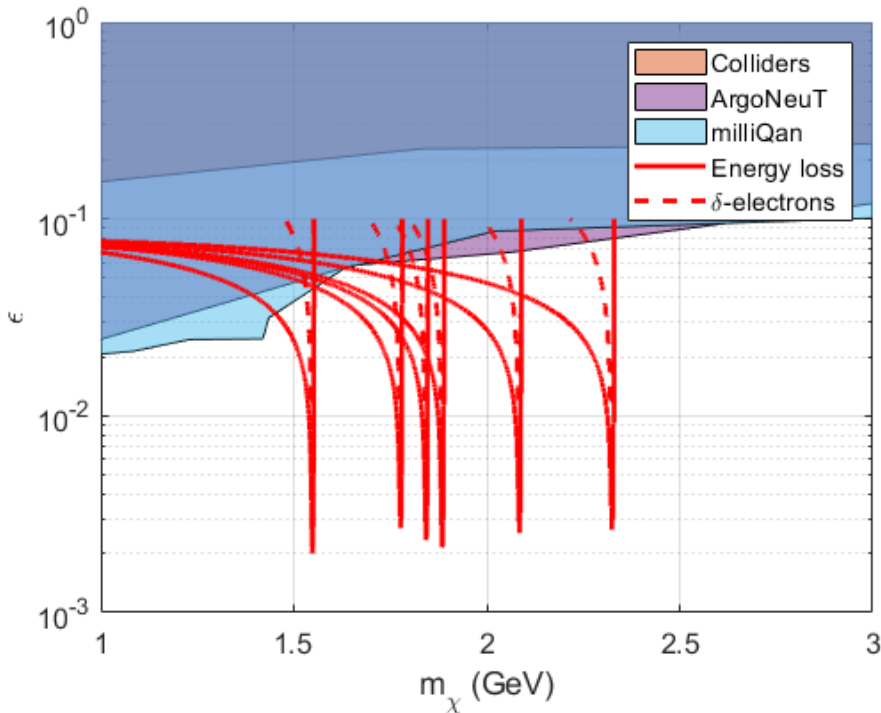


Figure 3: The regions to be probed at 95% CL with $e^+e^- \rightarrow \chi\chi$ and non-relativistic MCP signatures in the tracker after one year of operation following the scientific program of $c\text{-}\tau$ factory <https://sct.inp.nsk.su>. The smallest charge to be tested at different thresholds is somewhat different because of somewhat different luminosity there. The total collision statistics for one year is 1000 fb^{-1} . The shaded regions are excluded at 95% CL with searches undertaken by collaborations ArgoNeuT [23], milliQan [24], and terminated colliders [17].

\sqrt{s}, GeV	3.097	3.554	3.686	3.770	4.170	4.650
$\mathcal{L}_0, \text{fb}^{-1}$	300	50	150	300	100	100

Table 1: Energies, at which Super Charm–Tau factory data will be collected and integrated luminosity over these energies.

In this respect the ”standard” technique of searches for missing energy (carried away by MCPs), where the number of events scales as ϵ^2 is more promising, though it suffers from (ir)reducible background (see e.g. study of missing energy signature for $\tau\text{-}c$ factory [27]), which is absent in our case. The most attractive feature of our method is that we use the appearance as the signature, which immediately reveals the identity of new particles produced in collisions, while the missing energy is blind to its cause.

We thank A. Bondar, S. Demidov, S. Gninenko and I. Logashenko for the valuable discussions. The work on the expected signal coming from ionization energy loss of millicharged particles is supported by the Russian Science Foundation RSF grant 21-12-00379. The work of D. K. on the expected signal coming from δ -electrons is supported by the Foundation for

the Advancement of Theoretical Physics and Mathematics “BASIS”.

References

- [1] L. J. Hall, K. Jedamzik, J. March-Russell, and S. M. West, “Freeze-In Production of FIMP Dark Matter,” *JHEP* **03** (2010) 080, [arXiv:0911.1120 \[hep-ph\]](#).
- [2] N. Bernal, M. Heikinheimo, T. Tenkanen, K. Tuominen, and V. Vaskonen, “The Dawn of FIMP Dark Matter: A Review of Models and Constraints,” *Int. J. Mod. Phys. A* **32** no. 27, (2017) 1730023, [arXiv:1706.07442 \[hep-ph\]](#).
- [3] P. Agrawal *et al.*, “Feebly-interacting particles: FIPs 2020 workshop report,” *Eur. Phys. J. C* **81** no. 11, (2021) 1015, [arXiv:2102.12143 \[hep-ph\]](#).
- [4] B. Holdom, “Two U(1)’s and Epsilon Charge Shifts,” *Phys. Lett. B* **166** (1986) 196–198.
- [5] H. Goldberg and L. J. Hall, “A New Candidate for Dark Matter,” *Phys. Lett. B* **174** (1986) 151.
- [6] S. L. Dubovsky, D. S. Gorbunov, and G. I. Rubtsov, “Narrowing the window for millicharged particles by CMB anisotropy,” *JETP Lett.* **79** (2004) 1–5, [arXiv:hep-ph/0311189](#).
- [7] A. Melchiorri, A. Polosa, and A. Strumia, “New bounds on millicharged particles from cosmology,” *Phys. Lett. B* **650** (2007) 416–420, [arXiv:hep-ph/0703144](#).
- [8] M. I. Dobroliubov and A. Y. Ignatiev, “MILLICHARGED PARTICLES,” *Phys. Rev. Lett.* **65** (1990) 679–682.
- [9] S. Davidson and M. E. Peskin, “Astrophysical bounds on millicharged particles in models with a paraphoton,” *Phys. Rev. D* **49** (1994) 2114–2117, [arXiv:hep-ph/9310288](#).
- [10] J. H. Chang, R. Essig, and S. D. McDermott, “Supernova 1987A Constraints on Sub-GeV Dark Sectors, Millicharged Particles, the QCD Axion, and an Axion-like Particle,” *JHEP* **09** (2018) 051, [arXiv:1803.00993 \[hep-ph\]](#).
- [11] Y. Bai, S. J. Lee, M. Son, and F. Ye, “Muon $g - 2$ from millicharged hidden confining sector,” *JHEP* **11** (2021) 019, [arXiv:2106.15626 \[hep-ph\]](#).
- [12] H. Liu, N. J. Outmezguine, D. Redigolo, and T. Volansky, “Reviving Millicharged Dark Matter for 21-cm Cosmology,” *Phys. Rev. D* **100** no. 12, (2019) 123011, [arXiv:1908.06986 \[hep-ph\]](#).
- [13] A. Aboubrahim, P. Nath, and Z.-Y. Wang, “A cosmologically consistent millicharged dark matter solution to the EDGES anomaly of possible string theory origin,” *JHEP* **12** (2021) 148, [arXiv:2108.05819 \[hep-ph\]](#).
- [14] G. Lanfranchi, M. Pospelov, and P. Schuster, “The Search for Feebly Interacting Particles,” *Ann. Rev. Nucl. Part. Sci.* **71** (2021) 279–313, [arXiv:2011.02157 \[hep-ph\]](#).
- [15] J. L. Feng *et al.*, “The Forward Physics Facility at the High-Luminosity LHC,” [arXiv:2203.05090 \[hep-ex\]](#).
- [16] S. Davidson, B. Campbell, and D. C. Bailey, “Limits on particles of small electric charge,” *Phys. Rev. D* **43** (1991) 2314–2321.
- [17] S. Davidson, S. Hannestad, and G. Raffelt, “Updated bounds on millicharged particles,” *JHEP* **05** (2000) 003, [arXiv:hep-ph/0001179](#).
- [18] Z. Liu and Y. Zhang, “Probing millicharge at BESIII via monophoton searches,” *Phys. Rev. D* **99** no. 1, (2019) 015004, [arXiv:1808.00983 \[hep-ph\]](#).
- [19] J. Liang, Z. Liu, Y. Ma, and Y. Zhang, “Millicharged particles at electron colliders,” *Phys. Rev. D* **102** no. 1, (2020) 015002, [arXiv:1909.06847 \[hep-ph\]](#).
- [20] Z. Liu, Y.-H. Xu, and Y. Zhang, “Probing dark matter particles at CEPC,” *JHEP* **06** (2019) 009, [arXiv:1903.12114 \[hep-ph\]](#).
- [21] **Particle Data Group** Collaboration, P. A. Zyla *et al.*, “Review of Particle Physics,” *PTEP* **2020** no. 8, (2020) 083C01.
- [22] E. A. Kuraev and V. S. Fadin, “On Radiative Corrections to $e^+ e^-$ Single Photon Annihilation at High-Energy,” *Sov. J. Nucl. Phys.* **41** (1985) 466–472.
- [23] **ArgoNeuT** Collaboration, R. Acciarri *et al.*, “Improved Limits on Millicharged Particles Using the

- ArgoNeuT Experiment at Fermilab,” *Phys. Rev. Lett.* **124** no. 13, (2020) 131801, [arXiv:1911.07996 \[hep-ex\]](#).
- [24] A. Ball *et al.*, “Search for millicharged particles in proton-proton collisions at $\sqrt{s} = 13$ TeV,” *Phys. Rev. D* **102** no. 3, (2020) 032002, [arXiv:2005.06518 \[hep-ex\]](#).
- [25] R. Plestid, V. Takhistov, Y.-D. Tsai, T. Bringmann, A. Kusenko, and M. Pospelov, “New Constraints on Millicharged Particles from Cosmic-ray Production,” *Phys. Rev. D* **102** (2020) 115032, [arXiv:2002.11732 \[hep-ph\]](#).
- [26] G. Marocco and S. Sarkar, “Blast from the past: Constraints on the dark sector from the BEBC WA66 beam dump experiment,” *SciPost Phys.* **10** no. 2, (2021) 043, [arXiv:2011.08153 \[hep-ph\]](#).
- [27] Y. Zhang, W.-T. Zhang, M. Song, X.-A. Pan, Z.-M. Niu, and G. Li, “Probing invisible decay of dark photon at BESIII and future STCF via monophoton searches,” *Phys. Rev. D* **100** no. 11, (2019) 115016, [arXiv:1907.07046 \[hep-ph\]](#).